International Journal of Environmental Monitoring and Analysis
2022; 10(4): 96-103
http://www.sciencepublishinggroup.com/j/ijema
doi: 10.11648/j.ijema.20221004.11
ISSN: 2328-7659 (Print); ISSN: 2328-7667 (Online)

Development of an Empirical Ground Motion Prediction Model for North East India and Bangladesh Region

Tanzila Tabassum[1], Mehedi Ahmed Ansary[2]

[1]Transportation and Infrastructure Division, Applied Research Associates Inc. (ARA), Champaign, USA

[2]Department of Civil Engineering, Bangladesh University of Engineering and Technology, Dhaka, Bangladesh

Email address:
Ttabassum@ara.com (Tanzila Tabassum), ansary@ce.buet.ac.bd (Mehedi Ahmed Ansary)

To cite this article:
Tanzila Tabassum, Mehedi Ahmed Ansary, Development of an Empirical Ground Motion Prediction Model for North East India and Bangladesh Region. *International Journal of Environmental Monitoring and Analysis.* Vol. 10, No. 4, 2022, pp. 96-103.
doi: 10.11648/j.ijema.20221004.11

Received: March 24, 2022; **Accepted**: July 11, 2022; **Published**: August 29, 2022

Abstract: This article represents Ground-Motion Prediction Equations (GMPEs) for the North-East Indian region and Bangladesh derived from Indian Meteorological Department (IMD) strong motion database, following a standard regression approach. The database consists of 1608 three-component (North-South, East-West, and Vertical) time history records from 160 earthquakes having a magnitude between 2 to 8 from 2005 to 2017. The predicted ground parameters are expressed as a function of magnitude, distance (epicentral distance or hypocentral distance), and site category. The model uses a magnitude-independent shape according to geometrical spreading and anelastic attenuation for the attenuation relationships. The parametric GMPEs based on horizontal and vertical ground motions (peak ground acceleration, peak ground velocity) and spectral values (0.3 s, 1.0 s & 2.0 s.) have been developed in this study for rock, soft rock, and firm soil sites. The predictive values of horizontal and vertical components for firm soil sites are larger than those of soft rock and rock sites under the same conditions for a given earthquake event. Moreover, this study compares the effects of near-field earthquakes with far-field earthquakes and reveals that near-field earthquakes amplify more than far-field ones. This research also explains that the developed attenuation curves are depth and magnitude-independent and have no distance dependency.

Keywords: Ground Motion Prediction Equation, Regression Approach, Horizontal and Vertical Component, Spectral Value

1. Introduction

Earthquakes cause catastrophic destruction to civil infrastructure, including slides, cracks, and building failures, causing significant losses to human beings since the beginning of history [15]. The availability of more observation stations and high-quality data from the recently established global digital seismic network is essential to analyze, interpret present earthquakes, and predict future earthquakes hazard [31]. The epicenter and depth of the earthquakes and local site conditions play a vital role in seismic hazard analysis of civil infrastructure [22, 25]. Prediction of shaking intensity in future earthquakes plays an important role in seismic risk assessment that involves reliable data selection and proper ways to process [14].

Ground-motion prediction equations (GMPEs) are a function of distance (epicentral or hypocentral), magnitude, and site classification [6]. Previously, it was proved that earthquake intensity had poor correlations with the ground acceleration [16]. Researchers converted earthquake intensity data into equivalent strong motion data (acceleration and velocity) to solve this problem [20]. Authors predicted peak ground acceleration (PGA), peak ground velocity (PGV), and 5%-damped pseudo-acceleration response spectra (ARS) for spectral periods up to 3.0 s [4]. However, most of the studies avoid the prediction of peak ground displacement (PGD) as this response is sensitive to the low-cut filters [9]. Attenuation relations were developed for peak horizontal acceleration and velocity for near-fault earthquakes [23]. Similarly, predicted ground motion equations considering point-source

simulations and extended-source distance metrics were presented in the literatures [5].

In this research, the predicted peak ground parameters are expressed as a function of moment magnitude, distance (epicentral and hypocentral distance), focal depth of the earthquakes, and site category (rock and firm soil). The current database consisted of a total of 160 earthquakes with around 1608 three-component, North-South (NS), East-West (EW), and Vertical seismic recordings from the North-East Indian Meteorological Department (IMD) network of instruments. The multistage regression method has been used to calibrate the ground motion prediction equations proposed by Joyner and Boore (1981) and Bommer and Akkar (2012) model [5, 23]. These two models can avoid the bias of considered parameters and can retain magnitude-independent shape curves. Moreover, these models can decouple the distance dependency of the acquired data from the magnitude dependency and show the relationship associated with magnitude and distance for available ground motion data. This research includes two GMPEs derived from the same dataset to demonstrate and observe the potential difference and effect on the prediction equation associated with a focal depth of earthquakes, distance, and local site conditions.

2. Recorded Database and Response Variables

The dataset used in this research for studying ground motion attenuation relationships consists of 160 earthquakes with around 1608 three-component, e.g., North-South (NS), East-West (EW), and Vertical seismic recordings from the IMD network of instruments. The database used in this study contains peak ground acceleration values of the earthquakes having fault distances within 1000 km. The available earthquake records have been primarily divided into three categories according to the soil's stiffness expressed by the average shear wave velocity in the upper 30 meters (V_{S30}) of the deposits [9, 10, 26]. The range of V_{S30} has been assigned according to different site categories, e.g., NEHRP categories [17] by rock sites (soil type A), soft rock (soil type B), and firm soil sites (soil type C). The range of V_{S30} has been taken between 700 to 1620 m/s, 375 to 700 m/s, and 200 to 375 m/s for rock sites, soft rock sites, and firm soil sites. Additionally, the earthquake records have been assembled per the focal depth, shallow depth (0-70 km), intermediate-depth (70–300 km), and deep focus (300–700 km) events [27, 29]. These earthquakes are also classified into two categories concerning epicentral distance: near field (<60 km) and far-field earthquakes (60-1000 km) [21]. Table 1 shows the relevant information on the available dataset used in this study.

Table 1. *Summary of the available dataset used in this study.*

No. of earthquakes	160
No. of records	536
No. of three-component data	1608
No. of recording stations	163
Recorded data period	From 2005 to 2017
Magnitude range	2.3 - 7.8
Minimum intensity (larger of two horizontal components)	PGA ≥ 0.438 cm/s^2
Depth of the earthquake range	2 to 190 km
Epicentral distance	2 to 1000 km
Hypocentral distance (r)	9 to 1000 km
Shallow depth earthquakes	472 records
Intermediate depth earthquakes	52 records
Deep focus earthquake	0 records
Near field earthquakes	194 records
Far-field earthquakes	330 records
Rock sites (soil type A) 700< Vs_{30} <1620 m/s	273 records
Soft rock sites (soil type B) 375 < Vs_{30} <700 m/s	63 records
Firm soil sites (soil type C) 200 < V_{s30} < 375 m/s	200 records

3. Attenuation Model and Predictive Equations

Strong ground motion attenuation prediction models include variables, e.g., moment magnitude, distance, fault plane, frequency, and site classes [8]. This study utilized the attenuation equation of the form used by Joyner and Boore (1981) and Bommer and Akkar (2012) [5, 23]:

$$\log Y = b_1 + b_2\, r + b_3 M + b_4 \log r \pm \sigma \text{ (Joyner and Boore, 1981)} \quad (1)$$

$$\log Y = b_1 + b_2\, M + b_3 M^2 + (b_4 + b_5 M) \log r \pm \sigma \text{ (Bommer and Akkar, 2012)} \quad (2)$$

Where, Y = Ground Motion (acceleration, velocity, response spectrum); b_1, b_2, b_3, and b_4 = Regression coefficients; M = Moment magnitude; r = Hypocentral distance (km) = $\sqrt{epicentral\ distance^2 + depth^2}$; σ = Standard deviation.

To determine the coefficients and standard deviation from equations (1) and (2), the multiple regression method [9, 12, 19] has been used, and the predicted equations are for

different soil sites, distances and depths of earthquakes. These equations have been predicted by the response of the maximum value of the two consecutive horizontal components, e.g., the maximum of EW and NS value. Similar studies have also been performed by many authors [1, 2, 7]. However, the developed predictive models are considered to be more conventional, reliable, and acceptable, when the available data are consistent with the resulting equations, and the standard deviations are pretty low (near to zero) [30].

Attenuation models proposed by Joyner and Boore (1981), equation (1), and Bommer and Akkar (2012) [5, 23]; equation (2) are used in this study to fit the SGM data for different soil times and pseudo-spectral acceleration (PSA) values. This paper includes GMPEs for PGA, PGV and 5% damped PSA for periods 0.3 sec., 1 sec. and 2 sec. as a function of moment magnitude (M), hypocentral distance (r), and site class. The reasons behind choosing these spectral periods are that the spectral acceleration values less than 0.3 sec can generate de-amplification, but the spectral acceleration values can avoid this error between the time period of 0.3 sec to 2.0 sec [11, 24].

3.1. Regression Coefficients and Attenuation Models According to Soil Sites

Tables 2 and 3 show regression coefficients determined for rock, soft rock, and firm soil sites according to Joyner and Boore (1981) and Bommer and Akkar (2012) [5, 23] model, respectively. Here, b_1, b_2, b_3, b_4 are the coefficients for the independent variables, σ is the standard deviation (lesser value indicating good model), and correlation factor R^2 (higher value indicating good correlation between the parameters).

Table 2. *Regression coefficients for peak ground motions and spectral values using Joyner and Boore (1981) model.*

Soil Type	Y	b_1	b_2	b_3	b_4	σ	R^2
	$PGA_{max,h}$	0.80532	0.00029	0.36134	-0.92616	0.37057	0.35008
	$PGA_{max,v}$	0.70752	0.00033	0.38629	-1.06121	0.40904	0.36024
	$PGV_{max,h}$	0.23332	0.00025	0.28093	-0.64941	1.26125	0.02363
	$PGV_{max,v}$	0.29710	0.00037	0.24754	-0.75369	1.25565	0.02544
Rock site (soil	ARS_h (0.3s)	-1.97543	0.00032	-0.13774	0.57342	0.52654	0.18665
type A)	ARS_h (1.0s)	-2.36232	0.00006	-0.10470	0.69627	0.54808	0.19524
	ARS_h (2.0s)	-2.13429	0.00033	-0.14379	0.64215	0.53334	0.21353
	ARS_v (0.3s)	-2.48720	0.00000	-0.08348	0.61952	0.66552	0.12431
	ARS_v (1.0s)	-2.22717	0.00002	-0.05987	0.43130	0.64645	0.07373
	ARD_v (2.0s)	-2.39968	-0.00012	-0.10277	0.66317	0.60647	0.13431
	$PGA_{max,h}$	0.85098	-0.00015	0.00535	0.00330	0.36211	0.02108
	$PGA_{max,v}$	1.13017	-0.00012	-0.01378	-0.19721	0.37873	0.13376
	$PGV_{max,h}$	0.68508	0.00051	0.70206	-1.75986	1.37967	0.09074
	$PGV_{max,v}$	0.50595	0.00062	0.75025	-1.97377	1.37793	0.10559
Soft rock site	ARS_h (0.3s)	-4.75886	-0.00144	-0.11588	1.92896	0.52687	0.43246
(soil type B)	ARS_h (1.0s)	-4.23491	-0.00093	-0.16132	1.75496	0.53735	0.41404
	ARS_h (2.0s)	-4.42829	-0.00162	-0.08326	1.75920	0.60559	0.30960
	ARS_v (0.3s)	-4.91890	-0.00117	0.11758	1.34815	0.61267	0.33501
	ARS_v (1.0s)	-4.58649	-0.00126	0.05620	1.38152	0.60421	0.29356
	ARS_v (2.0s)	-4.52933	-0.00140	-0.07763	1.70359	0.71185	0.24662
	$PGA_{max,h}$	0.63296	-0.00062	0.43518	-0.84747	0.30658	0.49519
	$PGA_{max,v}$	0.56545	-0.00067	0.41255	-0.85580	0.34536	0.44610
	$PGV_{max,h}$	0.55935	0.00012	-0.23624	0.51760	1.30931	0.01283
	$PGV_{max,v}$	0.60381	0.00045	-0.30737	0.45938	1.30335	0.02197
Firm soil site	ARS_h (0.3s)	-3.13749	-0.00052	0.07768	0.70577	0.59477	0.17871
(soil type C)	ARS_h (1.0s)	-3.01049	-0.00062	0.09620	0.62204	0.57714	0.15254
	ARS_h (2.0s)	-2.81744	-0.00039	0.06788	0.58105	0.59339	0.13916
	ARS_v (0.3s)	-2.98277	-0.00054	0.09208	0.55851	0.67368	0.10135
	ARS_v (1.0s)	-3.57852	-0.00132	0.13989	0.82195	0.63922	0.16144
	ARS_v (2.0s)	-3.47533	-0.00105	0.07258	0.89599	0.64865	0.15442

Table 3. *Regression coefficients for peak ground motions and spectral values using (Bommer and Akkar, 2012) model.*

Soil Type	Y	b_1	b_2	b_3	b_4	b_5	σ	R^2
	$PGA_{max,h}$	0.01572	0.12328	0.07870	0.36183	-0.24825	0.36744	0.36340
	$PGA_{max,v}$	0.01549	0.12000	0.07856	0.18590	-0.23509	0.40893	0.36297
	$PGV_{max,h}$	0.60494	-0.35371	0.11282	0.39446	-0.20777	1.26228	0.02566
	$PGV_{max,v}$	1.44156	-0.67949	0.13472	0.16065	-0.16841	1.25704	0.02692
Rock site (soil	ARS_h (0.3s)	-0.77177	-0.34989	-0.01495	-0.23223	0.18542	0.52222	0.20325
type A)	ARS_h (1.0s)	-1.78714	-0.06227	-0.03513	0.01048	0.14537	0.54709	0.20153
	ARS_h (2.0s)	-1.21176	0.11363	-0.10098	-0.97367	0.35719	0.52387	0.24439
	ARS_v (0.3s)	-0.40104	-0.29914	-0.05029	-0.96401	0.33373	0.65031	0.16776
	ARS_v (1.0s)	-1.00245	-0.14135	-0.04011	-0.62087	0.22441	0.64084	0.09389
	ARS_v (2.0s)	-1.44359	0.17819	-0.10198	-0.91591	0.32913	0.59674	0.16555

Soil Type	Y	b_1	b_2	b_3	b_4	b_5	σ	R^2
	$PGA_{max,h}$	-1.03951	0.43648	-0.00609	0.75003	-0.15831	0.35600	.06986
	$PGA_{max,v}$	-0.37024	-0.05527	0.06002	1.35377	-0.28852	0.37289	0.17447
	$PGV_{max,h}$	3.33540	1.75415	-0.28412	-7.06906	0.98544	1.36980	0.11889
	$PGV_{max,v}$	3.66320	1.55550	-0.26343	-7.18629	0.98712	1.36914	0.13193
Soft rock site	ARS_h (0.3s)	-8.05363	-0.18245	0.17902	5.78057	-0.86842	0.54869	0.39492
(soil type B)	ARS_h (1.0s)	-5.78543	-0.39577	0.12960	4.18359	-0.54749	0.55305	0.38982
	ARS_h (2.0s)	-7.75328	-0.26043	0.20672	5.99454	-0.95871	0.63537	0.25292
	ARS_v (0.3s)	-8.52570	1.10434	-0.00028	2.74866	-0.41907	0.62856	0.31194
	ARS_v (1.0s)	-8.37287	0.83284	0.04477	3.50031	-0.55392	0.62239	0.26354
	ARS_v (2.0s)	-8.70253	0.93339	0.02394	3.67300	-0.55069	0.73259	0.21583
	$PGA_{max,h}$	-0.21224	0.61269	0.01595	-0.25977	-0.16759	0.31216	0.47932
	$PGA_{max,v}$	-0.42053	0.75202	-0.00915	-0.49652	-0.12559	0.34930	0.43628
	$PGV_{max,h}$	-1.39360	-1.20635	0.26292	4.58270	-0.79111	1.29721	0.03593
	$PGV_{max,v}$	-0.85807	-1.24603	0.22804	3.89521	-0.63607	1.29756	0.03559
Firm soil site	ARS_h (0.3s)	-2.79298	0.18648	-0.01987	0.28340	0.03770	0.60092	0.16592
(soil type C)	ARS_h (1.0s)	-2.60069	0.12248	-0.00349	0.35801	-0.00206	0.58558	0.13203
	ARS_h (2.0s)	-2.42870	0.18662	-0.02730	0.05313	0.06976	0.59730	0.13223
	ARS_v (0.3s)	-2.93939	0.58434	-0.08220	-0.45564	0.15258	0.67651	0.09846
	ARS_v (1.0s)	-5.14879	0.89017	-0.04817	0.97874	-0.14065	0.65152	0.13334
	ARS_v (2.0s)	-4.54408	0.43679	0.00066	1.39851	-0.18783	0.65994	0.12928

Here, subscript '*h*' and '*v*' denote coefficients for horizontal and vertical component, respectively.

Predicted peak horizontal acceleration decreases with the increase of hypocentral distances for rock sites and firm soil sites (Figure 1). Similar studies have been also observed in the literature [13]. In this study, the decay of predicted acceleration for soft rock sites has been excluded due to fewer data. Figure 1 shows that for a fixed earthquake magnitude, e.g., M = 6 or 7, the peak horizontal acceleration is dominant for Bommer and Akkar (2012) [5] attenuation model than Joyner and Boore (1981) [23] model. Moreover, the peak value of acceleration is more for firm soil and less for the rock site. This is because firm soil sites amplify more than rock sites [18]. The decay trend of the peak vertical acceleration follows the same trend as the horizontal component (Figure 2). Correspondingly, the acceleration's peak response in the vertical direction is larger for Bommer and Akkar (2012) [5] model than Joyner and Boore (1981) model [23] and more significant for firm soil than rock sites. From these Figures 1 and 2, it is also evident that the curves' shapes are independent of the earthquake magnitude. Peak horizontal and vertical acceleration had a very weak tendency to decrease with magnitude [3]. The predicted peak vertical acceleration decay rate is faster than the horizontal peak acceleration for any given moment magnitude. Moreover, the decay curves are steeper for Bommer and Akkar (2012) model [5] (Figure 1 (b) and 2 (b)) indicating faster decay and related to the higher frequency content in the ground motions [28]. However, the reason needs further investigation. Some of the predicted equations for the horizontal and vertical components of the earthquake ground motions after the regression method according to soil sites and corresponding authors are given below:

Rock sites (soil type A)

Joyner and Boore (1981)

$$\log A_{max,h} = 0.80532 + 0.00029*r + 0.36134*M - 0.92616*\log r \pm 0.37057\ \sigma \quad (3)$$

$$\log A_{max,v} = 0.70752 + 0.00033*r + 0.38629*M - 1.06121*\log r \pm 0.40904\ \sigma \quad (4)$$

Bommer and Akkar (2012)

$$\log A_{max,h} = 0.01572 + 0.12328*M + 0.07870*M^2 + (0.36183 - 0.24825*M) \log r \pm 0.36744\ \sigma \quad (5)$$

$$\log A_{max,v} = 0.01549 + 0.12000*M + 0.07856*M^2 + (0.18590 - 0.23509*M) \log r \pm 0.40893\sigma \quad (6)$$

Firm soil site (soil type C)

Joyner and Boore (1981)

$$\log A_{max,h} = 0.63296 - 0.00062*r + 0.43518*M - 0.84747*\log r \pm 0.30658\ \sigma \quad (7)$$

$$\log A_{max,v} = 0.56545 - 0.00067*r - 0.41255*M - 0.85580*\log r \pm 0.34536\ \sigma \quad (8)$$

Bommer and Akkar (2012)

$$\log A_{max,h} = -0.21224 + 0.61269*M - 0.01595*M^2 + (-0.25977 - 0.16759*M) \log r \pm 0.31216\ \sigma \quad (9)$$

$$\log A_{max,v} = -0.42053 + 0.75202*M - 0.00915*M^2 + (-0.49652 - 0.12559*M) \log r \pm 0.34930\ \sigma \quad (10)$$

Where *A* has units of *g* (*g* = 981 cm/sec^2). σ in the above expressions is equal to zero for mean values, and to one for 84

percentile and two for 98 percentile values of log A_{max}.

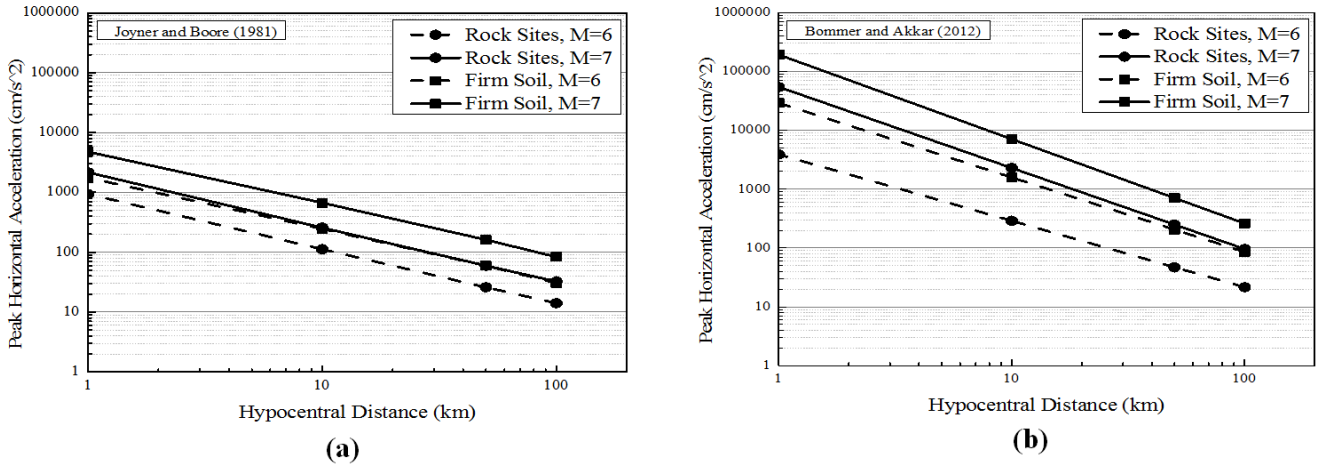

Figure 1. *Predicted peak horizontal acceleration: (a) Joyner and Boore (1981 [23]); (b) Bommer and Akkar (2012 [5]).*

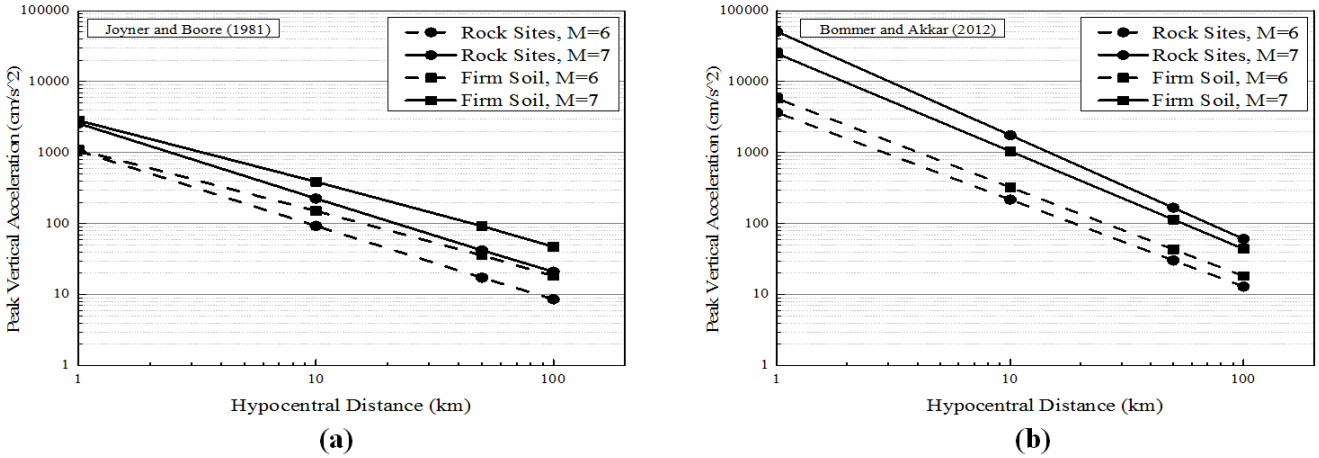

Figure 2. *Predicted peak vertical acceleration: (a) Joyner and Boore (1981) [23]; (b) Bommer and Akkar (2012) [5].*

3.2. Attenuation Models According to Depth and Epicentral Distance of Earthquakes

Attenuation models for shallow depth, near field, and far-field earthquakes are compared with each other for a fixed moment magnitude 6 and 7 having hypocentral distance up to 100 km, according to Joyner and Boore (1981) [23] and Bommer and Akkar (2012) model [5]. The prediction models for intermediate-depth earthquakes have been excluded in this study due to the data's lack of availability (Table 1). Figures 3 and 4 illustrate the attenuation models according to earthquakes' depths and epicentral distances. Here, the response is taken as the maximum value of the two horizontal components, e.g., maximum of NS and EW value.

Figure 3 (a) and (b) represent a comparison of all recorded data with the available data categorized into shallow depth with all data recorded according to Joyner and Boore (1981) [23] and Bommer and Akkar (2012) model [5] respectively. Whereas Figures 4 (a) and (b) represent the comparison of available near and far field earthquake data by Joyner and Boore (1981) [23] and Bommer and Akkar (2012) model [5]. The predicted attenuation model for all earthquake data (without any categorization) corresponding to the authors is given below:

$$\log A_{max,h} = 0.45612 - 0.00027*r + 0.39353*M - 0.73977*\log r \pm 0.3547\ \sigma \text{ (Joyner and Boore, 1981)} \quad (11)$$

$$\log A_{max,h} = 0.12628 + 0.44816*M + 0.00922*M^2 + (-0.47679 - 0.07301*M) \log r \pm 0.3552\ \sigma \text{ (Bommer and Akkar, 2012)} \quad (12)$$

The standard deviation for Joyner and Boore (1981) model [23] is ± 0.3547 and ±0.3552 for Bommer and Akkar (2012) model [5] which are satisfactory low. The correlation factors are 0.3461 and 0.3456, respectively. Standard deviation and correlation values signify that both models are reliable and acceptable. Adding to it, equation 13 and 14 show the attenuation model for shallow depth earthquakes of this study. The correlation factors for equation 13 (Joyner and Boore, 1981) [23] and equation 14 Bommer and Akkar (2012) [5] are 0.3541 and 0.3547 respectively.

$$\log A_{max,h} = 0.5091 - 0.00028*r + 0.40234*M - 0.79477*\log r \pm 0.3615\ \sigma \quad (13)$$

$$\log A_{max,h} = 0.29059+0.3826*M+0.01918*M^2+(-0.4733 - 0.0841*M) \log r \pm 0.36177\ \sigma \quad (14)$$

Predicted attenuation equations for the near field (equation 15-16), far-field earthquakes (equation 17-18) according to Joyner and Boore (1981) model [23] and Bommer and Akkar (2012) model [5] are as below:

Near field

$$\log A_{max,h} = 0.71197 + 0.00016*r + 0.44369*M - 1.0632*\log r \pm 0.3836\ \sigma \text{ (Joyner and Boore, 1981)} \quad (15)$$

$$\log A_{max,h} = 1.39947 + 0.06468*M + 0.04979*M^2 + (-0.98178 - 0.01794*M) \log r \pm 0.3826\sigma \text{ (Bommer and Akkar, 2012)} \quad (16)$$

Far-field

$$\log A_{max,h} = 0.5355 - 0.00032*r + 0.35229*M - 0.66913*\log r \pm 0.3346\ \sigma \text{ (Joyner and Boore, 1981)} \quad (17)$$

$$\log A_{max,h} = 0.41067 + 0.39414*M + 0.009*M^2 + (-0.53344 - 0.06083*M) \log r \pm 0.3358\ \sigma \text{ (Bommer and Akkar, 2012)} \quad (18)$$

From the results of Figure 3, it is perceived that the attenuation curves are magnitude independent for shallow depth earthquakes. For both models, shallow depth earthquake equations provide the same peak ground prediction value for magnitudes 6 and 7. Therefore, shallow depth earthquakes do not affect the attenuation models for both models for the current database. It would be more realistic if the present analysis could be performed for intermediate and deep focused earthquakes. It could also be mentioned that the slope of the Bommer and Akkar (2012) model [5] is relatively higher than Joyner and Boore (1981) model [23], indicating a faster decay rate.

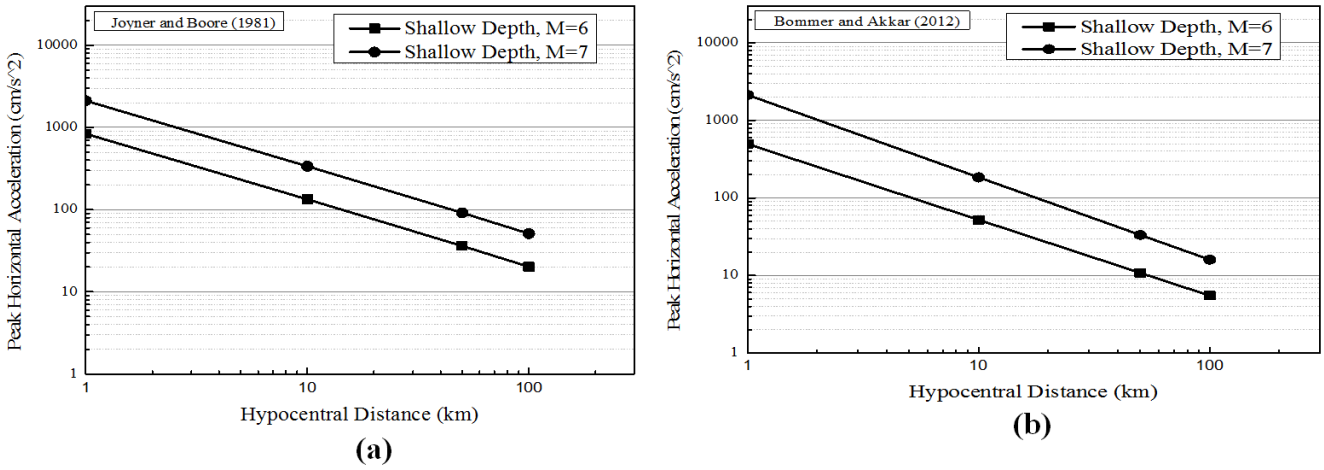

Figure 3. *Comparison of predicted horizontal PGA attenuation curves with the depth of earthquakes (a) Joyner and Boore (1981) [23], (b) Bommer and Akkar (2012) [5].*

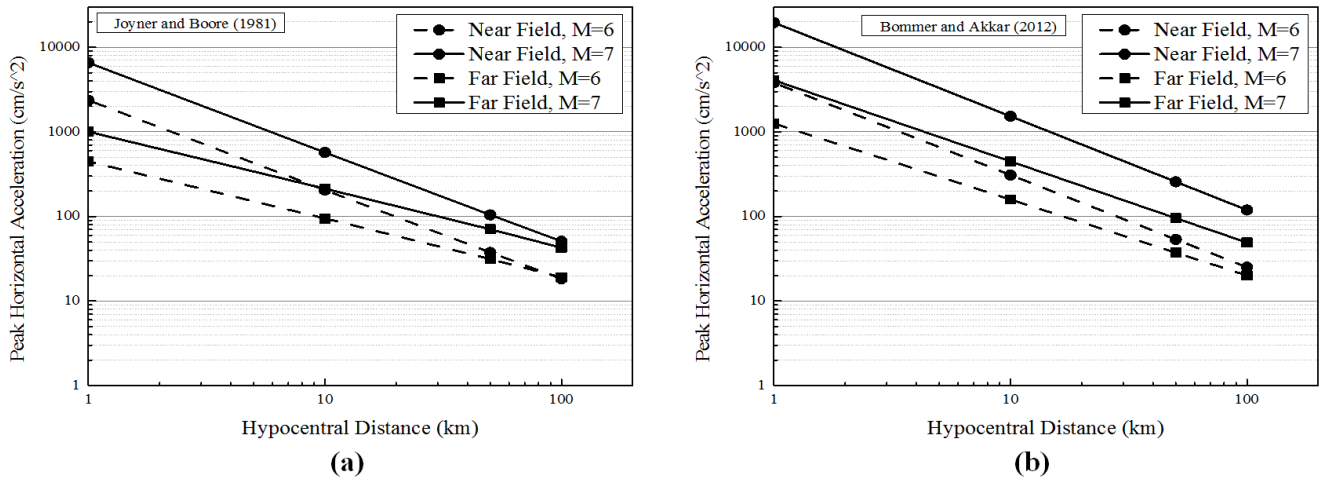

Figure 4. *Comparison of predicted horizontal PGA attenuation curves (a) Joyner and Boore (1981) [23], (b) Bommer and Akkar (2012) [5].*

Similarly, near field and far-field earthquake models are magnitude independent (Figure 4). Both amplification and decaying behavior are more rapid for predicted near field acceleration values than far-field values regardless of the accounted two models. Higher amplification is observed for Bommer and Akkar (2012) model [5] for a specific magnitude event, e.g., magnitude 6 or 7. It could also be mentioned that the near and far-field attenuation model behaves likewise at a larger hypocentral distance. Therefore, Figure 4 illustrates that epicentral distance has little influence in the predictive attenuation models. Both models have similar decay trends at a larger hypocentral distance, and their values are close enough. Similar results can be observed in the analysis performed by other authors [32]. They studied the near and far-field earthquake behavior and established that far-field earthquakes generate low amplitude waves than near field events.

4. Conclusion

The present study illustrates the ground motion prediction equation for the North-East Indian region and Bangladesh as a parameter of PGA, PGV, ARS for both horizontal and vertical directions. Predicted attenuation models for different soil sites, focal depth of the earthquakes, and epicentral distance are represented with respect to hypocentral distance and magnitude. This study affirms that firm soil sites' predictive values are larger than rock sites with the same conditions for a given earthquake event. Attenuation curves for both Joyner and Boore (1981) [23] and Bommer and Akkar (2012) [5] models are magnitude-independent, showing no change in the shapes. Furthermore, the predicted models' curves decay linearly with distance. However, predictive equations are sometimes governed by epicentral distance but not by the depth of the earthquake. The predicted results are found to be consistent with the available data with a relatively low standard deviation. This study does not incorporate any physical model and does not permit extrapolation beyond the obtained dataset range. This might be a limitation of this study. When the strong ground motion data over the entire observed area becomes plentiful, this limitation will become less critical. More observation stations need to be established to obtain high-quality seismic data for a better interpretation of earthquake data. This study provides a new idea to consider the attenuation relationships to be used in the North-East Indian region and Bangladesh.

References

[1] Ambraseys, N., Douglas, J., Sarma, S., and Smit, P. (2005). "Equations for the estimation of strong ground motions from shallow crustal earthquakes using data from Europe and the Middle East: horizontal peak ground acceleration and spectral acceleration". *Bulletin of Earthquake Engineering, 3* (1), 1-53.

[2] Ambraseys, N. N., Simpson, K. u., and Bommer, J. J. (1996). "Prediction of horizontal response spectra in Europe". *Earthquake engineering & structural dynamics, 25* (4), 371-400.

[3] Anderson, J. G., and Lei, Y. (1994). "Nonparametric description of peak acceleration as a function of magnitude, distance, and site in Guerrero, Mexico". *Bulletin of the seismological Society of America, 84* (4), 1003-1017.

[4] Bindi, D., Massa, M., Luzi, L., Ameri, G., Pacor, F., Puglia, R., and Augliera, P. (2014). "Pan-European ground-motion prediction equations for the average horizontal component of PGA, PGV, and 5%-damped PSA at spectral periods up to 3.0 s using the RESORCE dataset". *Bulletin of Earthquake Engineering, 12* (1), 391-430.

[5] Bommer, J. J., and Akkar, S. (2012). "Consistent source-to-site distance metrics in ground-motion prediction equations and seismic source models for PSHA". *Earthquake Spectra, 28* (1), 1-15.

[6] Bommer, J. J., Douglas, J., Scherbaum, F., Cotton, F., Bungum, H., and Fäh, D. (2010). "On the selection of ground-motion prediction equations for seismic hazard analysis". *Seismological research letters, 81* (5), 783-793.

[7] Bommer, J. J., Douglas, J., and Strasser, F. O. (2003). "Style-of-faulting in ground-motion prediction equations". *Bulletin of Earthquake Engineering, 1* (2), 171-203.

[8] Bommer, J. J., Stafford, P. J., and Alarcón, J. E. (2009). "Empirical equations for the prediction of the significant, bracketed, and uniform duration of earthquake ground motion". *Bulletin of the seismological Society of America, 99* (6), 3217-3233.

[9] Boore, D. M., and Atkinson, G. M. (2008). "Ground-motion prediction equations for the average horizontal component of PGA, PGV, and 5%-damped PSA at spectral periods between 0.01 s and 10.0 s". *Earthquake Spectra, 24* (1), 99-138.

[10] Borcherdt, R. D. (1994). "Estimates of site-dependent response spectra for design (methodology and justification)". *Earthquake Spectra, 10* (4), 617-653.

[11] Bozorgnia, Y., and Niazi, M. (1993). "Distance scaling of vertical and horizontal response spectra of the Loma Prieta earthquake". *Earthquake engineering & structural dynamics, 22* (8), 695-707.

[12] Brillinger, D. R., and Preisler, H. K. (1984). "An exploratory analysis of the Joyner-Boore attenuation data". *Bulletin of the seismological Society of America, 74* (4), 1441-1450.

[13] Campbell, K. W. (1981). "Near-source attenuation of peak horizontal acceleration". *Bulletin of the seismological Society of America, 71* (6), 2039-2070.

[14] Chaulagain, H., Rodrigues, H., Silva, V., Spacone, E., and Varum, H. (2015). "Seismic risk assessment and hazard mapping in Nepal". *Natural Hazards, 78* (1), 583-602.

[15] Coburn, A., and Spence, R. (2003). *Earthquake protection*: John Wiley & Sons.

[16] Cornell, C. A., Banon, H., and Shakal, A. F. (1979). "Seismic motion and response prediction alternatives". *Earthquake engineering & structural dynamics, 7* (4), 295-315.

[17] Crouse, C., and McGuire, J. (1996). "Site response studies for purpose of revising NEHRP seismic provisions". *Earthquake Spectra, 12* (3), 407-439.

[18] Darragh, R. B., and Shakal, A. F. (1991). "The site response of two rock and soil station pairs to strong and weak ground motion". *Bulletin of the seismological Society of America, 81* (5), 1885-1899.

[19] Graizer, V., and Kalkan, E. (2007). "Ground motion attenuation model for peak horizontal acceleration from shallow crustal earthquakes". *Earthquake Spectra, 23* (3), 585-613.

[20] Hasegawa, H., Basham, P., and Berry, M. (1981). "Attenuation relations for strong seismic ground motion in Canada". *Bulletin of the seismological Society of America, 71* (6), 1943-1962.

[21] Heydari, M., and Mousavi, M. (2015). "The comparison of seismic effects of near-field and far-field earthquakes on relative displacement of seven-storey concrete building with shear wall". *Current World Environment, 10* (Special Issue), 40.

[22] Idriss, I. (1991). "Earthquake ground motions at soft soil sites".

[23] Joyner, W. B., and Boore, D. M. (1981). "Peak horizontal acceleration and velocity from strong-motion records including records from the 1979 Imperial Valley, California, earthquake". *Bulletin of the seismological Society of America, 71* (6), 2011-2038.

[24] Joyner, W. B., and Boore, D. M. (1982). *Prediction of earthquake response spectra*: US Geological Survey Open-file report.

[25] Liao, Y., and Meneses, J. (2013). "Engineering characteristics of ground motion records from the 2010 Mw 7.2 El Mayor–Cucapah earthquake in Mexico". *Earthquake Spectra, 29* (1), 177-205.

[26] Nakamura, Y. (1989). "A method for dynamic characteristics estimation of subsurface using microtremor on the ground surface". *Railway Technical Research Institute, Quarterly Reports, 30* (1).

[27] Pérez, O. J. (1999). "Revised world seismicity catalog (1950-1997) for strong (Ms≥6) shallow (h≤70 km) earthquakes". *Bulletin of the seismological Society of America, 89* (2), 335-341.

[28] Rathje, E. M., Faraj, F., Russell, S., and Bray, J. D. (2004). "Empirical relationships for frequency content parameters of earthquake ground motions". *Earthquake Spectra, 20* (1), 119-144.

[29] Rehman, K., Ali, W., Ali, A., Ali, A., and Barkat, A. (2017). "Shallow and intermediate depth earthquakes in the Hindu Kush region across the Afghan-Pakistan border". *Journal of Asian Earth Sciences, 148*, 241-253.

[30] Schoups, G., and Vrugt, J. A. (2010). "A formal likelihood function for parameter and predictive inference of hydrologic models with correlated, heteroscedastic, and non-Gaussian errors". *Water resources research, 46* (10).

[31] Stein, S., and Wysession, M. (2009). *An introduction to seismology, earthquakes, and earth structure*: John Wiley & Sons.

[32] Van Der Elst, N. J., and Brodsky, E. E. (2010). "Connecting near-field and far-field earthquake triggering to dynamic strain". *Journal of Geophysical Research: Solid Earth, 115* (B7).